

A Synthetic Photoactivated Protein to Generate Local or Global Ca²⁺ Signals

Elizabeth Pham,¹ Evan Mills,¹ and Kevin Truong^{1,2,*}

¹Institute of Biomaterials and Biomedical Engineering, University of Toronto, 164 College Street, Toronto, ON M5S 3G9, Canada

²Edward S. Rogers Sr. Department of Electrical and Computer Engineering, University of Toronto, 10 King's College Circle, Toronto, ON M5S 3G4, Canada

*Correspondence: kevin.truong@utoronto.ca

DOI 10.1016/j.chembiol.2011.04.014

SUMMARY

Ca²⁺ signals regulate diverse physiological processes through tightly regulated fluxes varying in location, time, frequency, and amplitude. Here, we developed LOVS1K, a genetically encoded and photoactivated synthetic protein to generate local or global Ca²⁺ signals. With 300 ms blue light exposure, LOVS1K translocated to Orai1, a plasma membrane Ca²⁺ channel, within seconds, generating a local Ca²⁺ signal on the plasma membrane, and returning to the cytoplasm after tens of seconds. With repeated photoactivation, global Ca²⁺ signals in the cytoplasm were generated to modulate engineered Ca²⁺-inducible proteins. Although Orai1 is typically associated with global store-operated Ca²⁺ entry, we demonstrate that Orai1 can also generate local Ca²⁺ influx on the plasma membrane. Our photoactivation system can be used to generate spatially and temporally precise Ca²⁺ signals and to engineer synthetic proteins that respond to specific Ca²⁺ signals.

INTRODUCTION

Through tightly regulated Ca²⁺ concentration fluxes varying in location, time, frequency, and amplitude, Ca²⁺ signals regulate diverse and distinct physiological processes, including cell development, proliferation, migration, secretion, gene transcription, as well as cardiac excitation (EX)-contraction coupling (Berridge et al., 2000, 2003). Because intracellular Ca²⁺ regulates so many different, often opposing, cellular processes, it raises the question of how a ubiquitous messenger like Ca²⁺ can elicit very fine-tuned specific responses—a conundrum referred to as the Ca²⁺ specificity problem (Parekh, 2007). Specificity can in part be explained by the coupling of Ca²⁺ sensors such as calmodulin (CaM) with Ca²⁺ channels to selectively distinguish between the local Ca²⁺ signals from the channel and global Ca²⁺ signals from the endoplasmic reticulum (ER) (Tadross et al., 2008). Different local Ca²⁺ microdomains at the plasma membrane (PM) regulate cell functions ranging from the activation of catabolic enzymes to generate intracellular messengers (short-term responses on the seconds timescale) to the regulation of gene expression (long-term responses on the minutes-

to-hours timescale) (Parekh, 2009). The ability to generate local and global Ca²⁺ signals would allow us to better study the Ca²⁺ specificity problem and to engineer synthetic proteins that respond to specific Ca²⁺ signals. Using light to generate these Ca²⁺ signals is particularly desirable because light causes minimal damage to live cells and has the potential for high temporal and spatial resolution.

Although Ca²⁺ signals can be generated by light-mediated “uncaging” of Ca²⁺ chelators and IP₃ (Ellis-Davies, 2007), light-sensitive proteins such as Channelrhodopsin-2 (ChR2) (Boyden et al., 2005; Nagel et al., 2003, 2005) and its engineered mutants (Airan et al., 2009) are more favorable optogenetic alternatives because they do not require exogenous chemicals, are genetically encodable, and thus, are suitable for in vivo studies (Gradinaru et al., 2010). ChR2 is a leaky proton pump from the green alga *Chlamydomonas reinhardtii* (Boyden et al., 2005; Nagel et al., 2003, 2005) that preferentially transports H⁺ into the cell with blue light stimulation, but it is also permeable to K⁺, Na⁺, and Ca²⁺ (Nagel et al., 2003). The leaky nature of ChR2 has been exploited to generate action potentials for manipulating neural circuitry (Boyden et al., 2005; Kravitz et al., 2010), such as triggering behavioral responses in *C. elegans* (Nagel et al., 2005) and restoring light sensitivity to mice retinal neurons suffering from photoreceptor degeneration (Bi et al., 2006), as well as light-induced stimulation of heart muscles in mice (Brueggemann et al., 2010). Nevertheless, the drawbacks of using ChR2 to generate Ca²⁺ signals are: first, that it is not selective for Ca²⁺; and second, that it is most permeable to H⁺, and repeated exposure will decrease intracellular pH (Feldbauer et al., 2009).

To address the Ca²⁺ nonspecificity and intracellular pH problems of using ChR2 to generate Ca²⁺ signals, we developed a photoactivated means of triggering a local Ca²⁺ influx through Orai1 channels by recruitment of a stromal interaction molecule 1 (Stim1) C-terminal fragment. Previous studies have shown high Ca²⁺ selectivity through Orai1 (also known as calcium release-activated calcium channel protein 1) mediated by transmembrane helices forming specific binding sites for Ca²⁺ (McNally et al., 2009; Zhou et al., 2010). Stim1 and Orai1 synergistically activate store-operated Ca²⁺ entry (SOCE), a predominant mechanism used to replenish Ca²⁺ levels when intracellular stores are depleted (Varnai et al., 2009). Interestingly, expression of soluble C-terminal fragments of Stim1 can fully activate Orai1 channels independent of store depletion and puncta formation (Schindl et al., 2009). By fusing a Stim1 C-terminal fragment (233–450) to a LOV2 domain (Harper et al., 2004; Salomon et al., 2000), a light-responsive domain from phototropin-1, we

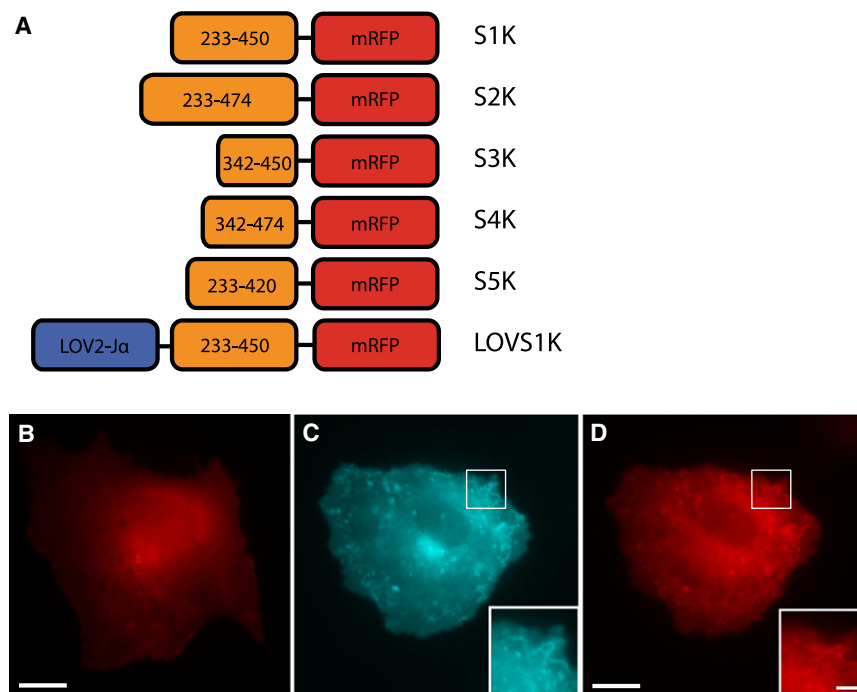


Figure 1. Stim1 Fragments Colocalized with Orai1Ceru

(A) Stim1 fragments S1K (233–450), S2K (233–474), S3K (342–450), S4K (342–474), and S5K (233–420) were fused to mRFP. S1K was subsequently fused to a LOV2-J α domain.

(B) S1K expressed alone in Cos-7 cells remained cytoplasmic.

(C and D) When coexpressed with Orai1Ceru (C), S1K localized to Orai1Ceru at the PM (D). For each construct, three experiments were performed, and ten of ten cells were observed. Scale bar represents 30 μ m; inset scale bar represents 9 μ m. Images are false color: Orai1Ceru, cyan; Stim1 fragments, red.

See also Figure S1.

created LOVS1K, a photosensitive synthetic protein that reversibly translocates to Orai1 channels to generate a local Ca²⁺ signal on the PM or a global Ca²⁺ signal in the cytoplasm with repeated photostimulation.

RESULTS

Stim1 Fragments Were Constitutively Localized with Orai1

A selection of C-terminal fragments from Stim1 corresponding to those reported in literature (Schindl et al., 2009), i.e., S1K (233–450), S2K (233–474), S3K (342–450), S4K (342–474), and S5K (233–420), was fused to a monomeric red fluorescent protein (mRFP), and all except S5K colocalized with Orai1Ceru, a fusion protein of full-length Orai1 with Cerulean, a cyan fluorescent protein (CFP) (Figure 1A). In the literature the C-terminal fragments of Stim1 were shown to colocalize and fully activate Orai1 channels independent of store depletion and puncta formation (Schindl et al., 2009). Structurally, a putative C-terminal coiled-coil domain on Orai1 couples with these coiled-coil fragments from Stim1 (Calloway et al., 2010). When our mRFP fusions of these fragments were expressed in Cos-7 cells alone, all remained cytoplasmic ($n = 10/10$ cells for each construct) (Figure 1B; see Figure S1 available online). In some cells there was some localization to the PM, but this is likely due to endogenous Orai1 expression in Cos-7 cells. When coexpressed with Orai1Ceru, all fragments except S5K were localized with Orai1Ceru ($n = 10/10$ cells for each construct) (Figures 1C and 1D; Figure S1). Consistent with reported studies, a Stim1 fragment truncated beyond residue 420 (S5K) failed to interact with Orai1Ceru (Figure S1) (Schindl et al., 2009). S1K–S4K contain both the small basic sequence (384–386) shown to be important for electrostatically interacting with the acidic coiled-

coil region of Orai1 and the essential second coiled-coil domain of Stim1 (residues 344–442) necessary to activate Orai1 (Calloway et al., 2010; Frischauf et al., 2009). Taken together, these results indicate that S1K–S4K specifically target Orai1Ceru. Although the expression pattern of Orai1Ceru was expected to be clearly PM bound, the expression pattern

observed was not exclusively at the PM. Additionally, Stim1-fragment localization did not completely coincide with the expression pattern of Orai1Ceru. The observed expression pattern of Orai1Ceru may also include Orai1 proteins that are in different folding states, trapped in endosomes, or undergoing vesicular trafficking, so that binding sites are either not accessible or occupied by endogenous proteins (Woodard et al., 2008; Yu et al., 2009, 2010). Inset images have been used to better highlight where colocalization was more apparent.

Fusion of LOV2-J α Allowed Photoactivated Recruitment of Stim1 Fragments to Orai1

By fusing S1K–S4K to the LOV2 domain of phototropin-1 (Harper et al., 2004; Salomon et al., 2000), fusion proteins (LOVS1K–LOVS4K) were created, and when coexpressed with Orai1Ceru, LOVS1K and LOVS2K translocated to Orai1Ceru within several seconds after 300 ms exposure to blue light. The LOV2 domain has recently been fused to GTPase Rac1 (Wu et al., 2009) and *E. coli* trp repressor protein (Strickland et al., 2008) to create photoactivated switches. In the dark state, LOV2 binds a flavin chromophore and compactly interacts with a C-terminal helix (J α). Under blue light illumination, photon absorption forms a covalent cysteinyl-flavin bond that causes J α to dissociate and unwind (Strickland et al., 2008). We hypothesized that LOV2-J α interaction in the dark state would sterically prevent interaction between Orai1Ceru and LOVS1K–LOVS4K, and release this inhibition when photostimulated (bright state) to restore Orai1Ceru interaction.

When expressed without Orai1Ceru, LOVS1K–LOVS4K remained in the cytoplasm in both the dark and bright states ($n = 10/10$ cells for each construct) (Figure 2A; Figure S2). Similarly, when coexpressed with Orai1Ceru and imaged only through the mRFP channel (580 ± 20 nm), LOVS1K,

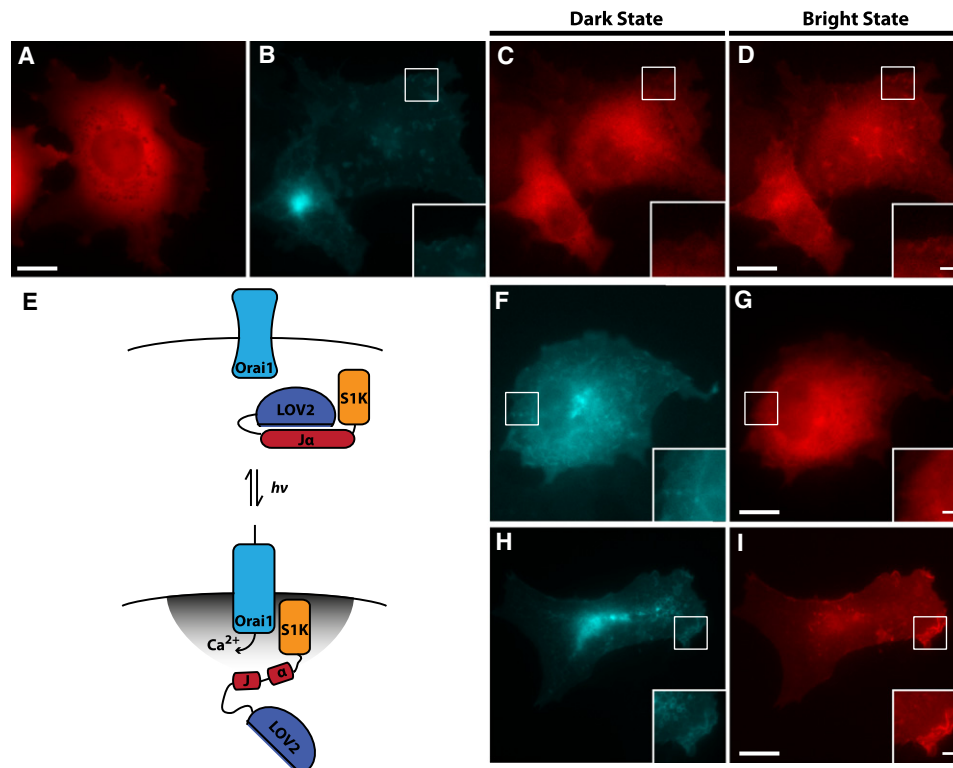


Figure 2. Photoactivated LOVS1K Localized to Orai1CerU

(A) LOVS1K expressed alone in Cos-7 cells was cytoplasmic ($n = 3$ experiments and 10/10 observed cells).

(B–D) When coexpressed with Orai1CerU (B), LOVS1K remained cytoplasmic in the dark state (C) and translocated to Orai1CerU on the PM in the bright state (D) ($n = 5$ experiments and 25/25 observed cells).

(E) Cartoon representation of LOVS1K photoactivation of Orai1CerU.

(F and G) darkLOVS1K remained cytoplasmic and did not colocalize with Orai1CerU in the bright state ($n = 2$ experiments and 10/10 observed cells).

(H and I) brightLOVS1K remained prelocalized with Orai1CerU in both the dark and bright states ($n = 2$ experiments and 10/10 observed cells). $h\nu$, blue light illumination. Scale bars represent 30 μm ; inset scale bars represent 9 μm . Images are false color: Orai1CerU, cyan; Stim1 fragments, red.

See also Figures S2 and S3.

LOVS2K, and LOVS3K remained in the cytoplasm. With 300 ms exposure to blue light (438 ± 24 nm), LOVS1K ($n = 25/25$ cells) and LOVS2K ($n = 12/12$ cells) localized with Orai1CerU at the PM within 5 s (Figures 2B–2D; Figure S2). LOVS3K was not recruited to Orai1CerU, even under 1 min of constant blue light illumination ($n = 12/12$ cells) (Figure S2). Despite S3K corresponding to the reported minimal sequence necessary to constitutively interact with and activate Orai1 (Schindl et al., 2009), the fusion of LOVS2K-J α appears to interfere with Orai1 binding in both the dark and bright states. In contrast the fusion of LOVS4K-J α was unable to sterically block the interaction between LOVS4K and Orai1CerU, so LOVS4K was localized with Orai1CerU at the PM both in the dark and bright states ($n = 12/12$ cells) (Figure S2). These results demonstrate that LOVS1K and LOVS2K can be used as photoswitches, remaining cytoplasmic in the dark state and recruited to the PM in the bright state (Figure 2E). Because LOVS1K was the smallest fragment that can be photoactivated, it was chosen for further characterization. Thus, translocation of LOVS1K to Orai1CerU with blue light illumination was further verified in several cell lines, including HeLa, NIH 3T3, and HEK293 (Figure S3).

As controls, we fused S1K with two reported LOVS2 domain mutations that render LOVS2 domains either permanently bound to J α (Cys450Ala) or permanently unbound (Ile539Glu) (Salomon et al., 2000; Wu et al., 2009). These constructs were named darkLOVS1K and brightLOVS1K because they mimic the dark and bright states of LOVS2-J α , respectively. As expected, darkLOVS1K remained in the cytoplasm both in the absence and presence of blue light stimulation despite Orai1CerU coexpression, similar to LOVS1K in the dark state (Figures 2F and 2G). Also consistent with our expectations, brightLOVS1K was constitutively localized with Orai1CerU at the PM (Figures 2H and 2I). Photoactivated LOVS1K can only bind to unoccupied Orai1CerU at the time of photostimulation. In contrast the localization of brightLOVS1K reflects an accumulation of this binding with Orai1CerU. Hence, the localization of brightLOVS1K to Orai1CerU appears to be brighter than the bright state of LOVS1K, and blue light stimulation of brightLOVS1K did not result in any observable additional translocation. Taken together, these results demonstrate that the photoswitchability of LOVS1K is due to LOVS2-J α sterically blocking the interaction of S1K with Orai1CerU in the dark state. With blue light illumination, J α undocks from LOVS2 and unwinds, releasing S1K to restore

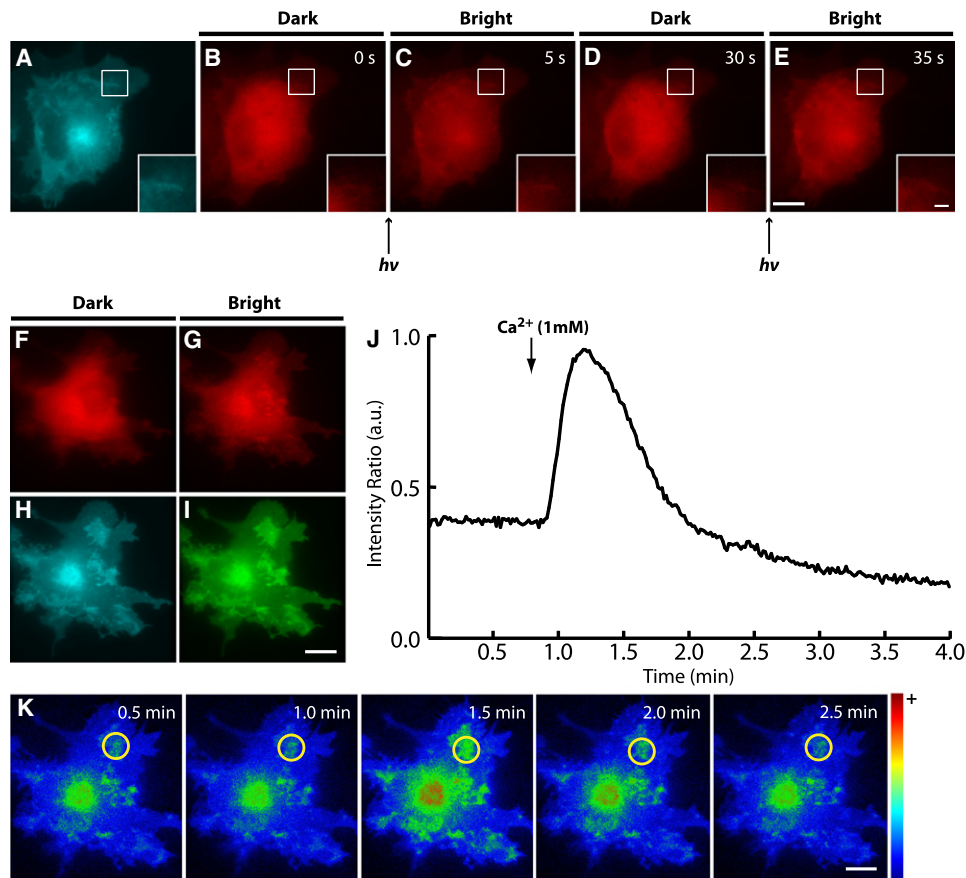


Figure 3. Photoactivated Translocation of LOVS1K to Orai1CerU Was Reversible, Can Be Repeated, and Caused a Local Ca²⁺ Signal on the PM

(A–E) When coexpressed with Orai1CerU (A), LOVS1K was initially cytoplasmic (dark state) (B). With 300 ms exposure to blue light, LOVS1K was translocated to Orai1CerU on the PM within 5 s (bright state) (C). After 30 s LOVS1K returned to the cytoplasm (D). A subsequent exposure to blue light retranslocated LOVS1K to Orai1CerU (E) ($n = 3/3$ experiments). *hν*, blue light illumination. Images are false color: Orai1CerU, cyan; LOVS1K, red.

(F–I) Cos-7 cells expressing LOVS1K (dark state, F; bright state, G), Orai1CerU (H), and pLynTNXL (I).

(J) A local Ca²⁺ signal was measured at the PM of Cos-7 cells using pLynTNXL FRET biosensor upon addition of 1 mM Ca²⁺ ($n = 9/9$ experiments). YFP/CFP intensity ratios presented as the percentage of maximum ratio change with 1 μ M ionomycin, minimum determined by addition of 1 mM EDTA. The CFP EX filter (438 ± 24 nm) was used to both photoactivate LOVS1K and excite pLynTNXL. Images are false color: red, LOVS1K; green, YFP channel EX of pLynTNXL; cyan, Orai1CerU and CFP channel EX of pLynTNXL.

(K) FRET intensity change of pLynTNXL corresponding to 1 mM Ca²⁺ addition in (J). Scale bars represent 30 μ m; inset scale bars represent 9 μ m. “+” and “–” indicate higher and lower ratios, respectively. FRET intensity change is measured at circled region.

See also Figure S3 and Movie S1.

interaction with Orai1CerU. The translocation of LOVS1K to Orai1CerU on the PM is reversible (Figure 3A; Movie S1). A 300 ms exposure to blue light recruits LOVS1K to Orai1CerU on the PM within seconds (<5 s). Within 10–30 s in the dark state, LOVS1K dissociates and returns to the cytoplasm. A subsequent photostimulation recruits LOVS1K back to Orai1CerU on the PM ($n = 3/3$ experiments) (Figures 3B–3E).

Colocalization Analysis

To quantify the comparison of colocalization between different LOV-Stim1 fragments with Orai1CerU, commonly used colocalization coefficients have been calculated (Tables 1 and 2). A number of methods to measure colocalization have been reported (Bolte and Cordelieres, 2006; Li et al., 2004; Manders et al., 1992; van Steensel et al., 1996). However, not all available

measures are suitable for assessing the colocalization of nonuniform, discrete protein localizations within a cell such as those seen with LOVS1K and Orai1CerU (Bolte and Cordelieres, 2006; van Steensel et al., 1996). Here, we report Pearson’s coefficient (PC), which is commonly used to compare the occurrence of colocalization (Bolte and Cordelieres, 2006). The accuracy of this colocalization analysis relies heavily on the signal to noise ratio, which can be improved post-acquisition using background subtraction and thresholding. In order to avoid user bias, Costes’ automatic thresholding was additionally used to calculate thresholded PC values (Costes et al., 2004) as well as van Steensel’s cross-correlation coefficients (CCFs) (van Steensel et al., 1996).

Colocalization coefficients were first calculated and compared for relevant control cases: PM-to-PM colocalization (i.e., two proteins localized at the PM such as pLyn-mRFP and pLyn-Ceru)

Table 1. Colocalization Coefficients for LOV-Stim1 Fragments—Whole-Cell Analysis

Whole-Cell Analysis	PC	PC with Costes' Thresholding	van Steensel's Peak CCF ^a	PC (% change)	PC with Costes' (% change)	van Steensel's Peak CCF (% change)
mRFP and pLyn-Ceru	0.743	0.722	0.763			
pLyn-mRFP and pLyn-Ceru	0.964	0.963	0.964	29.7	33.4	26.3
LOVS1K (dark)	0.830	0.826	0.830			
LOVS1K (bright)	0.886	0.883	0.887	6.7	6.9	6.9
LOVS2K (dark)	0.885	0.867	0.888			
LOVS2K (bright)	0.915	0.880	0.895	3.4	1.5	0.8
LOVS3K (dark)	0.917	0.887	0.917			
LOVS3K (bright)	0.917	0.896	0.918	0	1.0	0.1
LOVS4K (dark)	0.925	0.920	0.925			
LOVS4K (bright)	0.933	0.929	0.936	0.9	1.0	1.2
darkLOVS1K (dark)	0.865	0.812	0.872			
darkLOVS1K (bright)	0.878	0.820	0.880	1.5	1.0	0.9
brightLOVS1K (dark)	0.973	0.971	0.974			
brightLOVS1K (bright)	0.973	0.977	0.973	0	0.6	-0.1
Repeated Recruitment of LOVS1K to Orai1Ceru						
Time 0 s (dark)	0.916	0.912	0.921			
Time 5 s (bright)	0.942	0.938	0.947	2.8	2.9	2.8
Time 30 s (dark)	0.921	0.918	0.924	-2.2	-2.1	-2.4
Time 35 s (bright)	0.939	0.935	0.943	2.0	1.9	2.1

^aAll CCF values were statistically significant with van Steensel's R² values greater than 0.95.

versus cytoplasm-to-PM colocalization (i.e., one cytoplasmic protein and one PM-localized protein such as mRFP and pLyn-Ceru) (Figures S2M–S2P). Given the experimental setup, PC

values calculated for these control cases showed a difference of about 29.7% between PM-to-PM and cytoplasm-to-PM colocalization. Irregular colocalization patterns are particularly

Table 2. Colocalization Coefficients for LOV-Stim1 Fragments—ROI Analysis

ROI Analysis ^a	PC	PC with Costes' Thresholding	van Steensel's Peak CCF ^b	PC (% change)	PC with Costes' (% change)	van Steensel's Peak CCF (% change)
mRFP and pLyn-Ceru	0.612	0.588	0.612			
pLyn-mRFP and pLyn-Ceru	0.934	0.930	0.935	52.6	58.2	52.8
LOVS1K (dark)	0.579	0.549	0.638			
LOVS1K (bright)	0.758	0.762	0.761	30.9	38.8	19.3
LOVS2K (dark)	0.606	0.421	0.606			
LOVS2K (bright)	0.763	0.589	0.781	25.9	39.9	28.9
LOVS3K (dark)	0.915	0.889	0.916			
LOVS3K (bright)	0.927	0.916	0.932	1.3	3.0	1.7
LOVS4K (dark)	0.798	0.695	0.823			
LOVS4K (bright)	0.841	0.823	0.858	5.4	18.4	4.3
darkLOVS1K (dark)	0.878	0.844	0.889			
darkLOVS1K (bright)	0.881	0.843	0.885	0.3	-0.1	-0.4
brightLOVS1K (dark)	0.953	0.952	0.945			
brightLOVS1K (bright)	0.961	0.958	0.961	0.8	0.6	1.7
Repeated Recruitment of LOVS1K to Orai1Ceru						
Time 0 s (dark)	0.734	0.676	0.740			
Time 5 s (bright)	0.790	0.761	0.802	7.6	12.6	8.4
Time 30 s (dark)	0.778	0.720	0.791	-1.5	-5.4	-1.4
Time 35 s (bright)	0.807	0.761	0.817	3.5	5.7	3.3

^aAll regions of interest correspond to inset images.

^bAll CCF values were statistically significant with van Steensel's R² values greater than 0.95.

difficult to assess (van Steensel et al., 1996), so restricting the analysis to a region of interest helps to quantify discrete sites of colocalization, especially of nonuniform structures (Bolte and Cordelières, 2006; Costes et al., 2004). Using regions of interest of the same dimensions, the difference between the PM-to-PM and cytoplasm-to-PM colocalization was about 52.6%.

A similar comparison was done for acquired images, using both whole-cell analysis (Table 1) and regions of interest (corresponding to indicated inset images) (Table 2). Our whole-cell colocalization analysis showed a 6.7% increase in colocalization of LOVS1K and Orai1Ceru (30.9% increase for inset image) after photostimulation of LOVS1K. These results confirmed that LOVS1K becomes partially colocalized with Orai1Ceru at the PM upon photostimulation. This increase in colocalization was additionally confirmed with both thresholded PCs and van Steensel's CCF values. Colocalization coefficients also confirmed that there was minimal change in colocalization between the dark and bright states for the darkLOVS1K (1.5% increase, 0.3% for inset image) and brightLOVS1K (0% change, 0.8% increase for inset image) controls. These small changes in localization are potentially real because the LOV2 domain mutations reduce but do not completely abolish the response to light. Repeated photoactivation of LOVS1K showed a corresponding increase in colocalization to Orai1Ceru upon photostimulation of approximately 2.8% (7.6% increase for inset image), a decrease in colocalization in the dark state of approximately 2.2% (1.5% decrease for inset image), and a subsequent increase of approximately 2.0% (3.5% increase for inset image) upon a second photostimulation. These results confirm that the photoactivation of LOVS1K is reversible and can be repeatedly photostimulated.

Photoactivated Translocation of LOVS1K Caused a Local Ca²⁺ Signal on the PM

Using a Ca²⁺ biosensor with fast kinetics called TNXL (Heim and Griesbeck, 2004; Mank et al., 2006) and a PM-bound version named pLynTNXL, a local Ca²⁺ signal was measured at the PM when LOVS1K was recruited to Orai1Ceru by blue light stimulation. TNXL is a troponin-C-based Ca²⁺ biosensor that uses the fluorescence resonance energy transfer (FRET) between a CFP donor and yellow fluorescent protein (YFP) acceptor to measure intracellular Ca²⁺ changes as reflected in the ratio change between CFP and YFP emissions (EMs) (Figures S4A and S4B). TNXL was targeted to the PM using a common N-terminal localization peptide (GCIKSKGKDSA) (Inoue et al., 2005) to create pLynTNXL. As controls, TNXL and pLynTNXL were used to measure Ca²⁺ changes in Cos-7 cells upon addition of 1 μM thapsigargin (Tg) and 1 mM extracellular Ca²⁺. Tg causes a global increase in cytosolic Ca²⁺ by causing a depletion of ER Ca²⁺ stores. When Ca²⁺ is present in the extracellular medium, ER depletion causes a subsequent influx of extracellular Ca²⁺. Cells expressing either TNXL or pLynTNXL were imaged in Ca²⁺-free media. As expected, TNXL was able to measure both the global cytosolic Ca²⁺ increase upon addition of 1 μM Tg (release of ER Ca²⁺) and the influx of Ca²⁺ into the cytoplasm upon addition of 1 mM extracellular Ca²⁺. In contrast, pLynTNXL did not measure the Tg-induced increase in global cytosolic Ca²⁺ but was able to measure the influx of Ca²⁺ at the PM upon addition of extracellular Ca²⁺.

Thus, because the illumination wavelengths required to photoactivate LOV2-J α release and to excite the CFP donor protein are within the same range (438 ± 24 nm), blue light illumination facilitated both photoactivation of LOVS1K (and hence recruitment to Orai1Ceru) and FRET measurements. To avoid any LOVS1K-mediated Ca²⁺ influx while measuring the basal FRET ratio from TNXL, cells expressing TNXL, LOVS1K, and Orai1Ceru were first imaged in Ca²⁺-free media. Subsequent addition of 1 mM Ca²⁺ should result in an increase in FRET ratio corresponding to any LOVS1K-mediated Ca²⁺ influx. Upon addition of 1 mM Ca²⁺, no increase in global intracellular Ca²⁺ levels was observed with TNXL. However, the same experiment repeated with pLynTNXL showed a local Ca²⁺ signal (n = 9/9 experiments) (Figures 3F–3K). Similar local Ca²⁺ signals were observed in HeLa, NIH 3T3, and HEK293 cells (Figure S3). In contrast, Cos-7 cells expressing pLynTNXL and LOVS1K (without Orai1Ceru) did not show even a local Ca²⁺ signal (n = 3/3 experiments) (Figure S4C). Control cells expressing pLynTNXL alone or pLynTNXL with Orai1Ceru did not show a Ca²⁺ change upon addition of Ca²⁺ alone. Taken together, these observations confirm that Orai1Ceru photoactivation by LOVS1K recruitment generates a local Ca²⁺ influx through Orai1Ceru as opposed to a global cytoplasmic transient upon Ca²⁺ addition.

Repeated Photoactivation of LOVS1K Can Generate Global Ca²⁺ Signals in the Cytoplasm

LOVS1K was used to generate global Ca²⁺ signals in the cytoplasm to modulate two different engineered Ca²⁺-inducible proteins that demonstrate Ca²⁺-dependent protein translocation or cell morphology changes. Because recruitment of LOVS1K to Orai1Ceru generated a local Ca²⁺ influx, the repeated recruitment of LOVS1K should gradually accumulate into a global Ca²⁺ signal in the cytoplasm. To verify this, the global Ca²⁺ concentration was monitored in cells expressing TNXL, LOVS1K, and Orai1Ceru. Repeated photoactivation of LOVS1K (300 ms exposure every 30 s; n = 6/6 cells) showed a gradual increase in global Ca²⁺ in the presence of 1 mM extracellular Ca²⁺, reaching the intracellular Ca²⁺ concentration of approximately 500 nM after 40 min (Figure S4D). Although this timescale may not be appropriate for some global Ca²⁺ studies, these results nonetheless confirm the possibility of using the fast local Ca²⁺ signals from LOVS1K to generate a gradual global Ca²⁺ signal. Thus, LOVS1K was further used to confirm that such an accumulation of intracellular Ca²⁺ would be useful in modulating Ca²⁺-sensitive proteins. IELM-Venus is a synthetic Ca²⁺-inducible protein containing CaM-binding peptides that selectively localizes in the nucleoli in low Ca²⁺ conditions and translocates to the PM in high global Ca²⁺ conditions (Mills and Truong, 2010). Thus, the translocation of IELM-Venus from the nucleoli to the PM can be used as a reliable indicator of sustained high global Ca²⁺ concentrations (Mills and Truong, 2010). A clear translocation of IELM-Venus from the nucleoli to the PM was observed in Cos-7 cells coexpressing LOVS1K and Orai1Ceru within 3 hr of pulsed photostimulation (300 ms exposure every 10 s; n = 10/10 cells) (Figure 4C; Movie S4). A delay of 10 s between exposures was chosen because it would allow LOVS1K enough time to return to the cytoplasm. Under the same pulsed photostimulation conditions, this translocation was not observed in control cells expressing IELM-Venus alone (n = 5/5 cells)

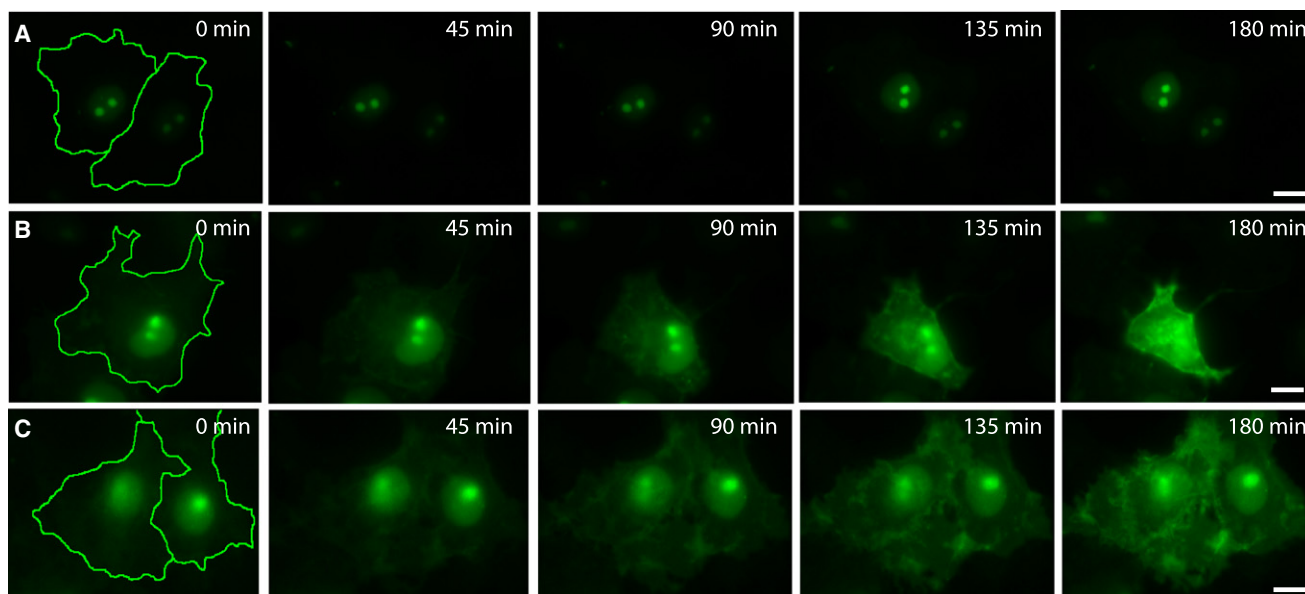


Figure 4. Translocation of IELM-Venus from the Nucleoli to the PM with Repeated Photoactivation of LOVS1K

(A) No translocation of IELM-Venus was observed in Cos-7 cells after 3 hr ($n = 2$ experiments and 5/5 observed cells).

(B) Translocation of IELM-Venus in ChR2-mCherry-expressing Cos-7 cells occurred within 3 hr of pulsed photostimulation; cell shrinkage was observed after 1 hr ($n = 2$ experiments and 5/5 observed cells).

(C) Translocation of IELM-Venus in LOVS1K- and Orai1Ceru-expressing Cos-7 cells occurred within 3 hr of pulsed photostimulation ($n = 3$ experiments and 10/10 observed cells). Scale bars represent 30 μm . Images are false color: IELM-Venus, green. Cell outlines highlighted for time zero.

See also [Movie S2](#), [Movie S3](#), and [Movie S4](#).

(Figure 4A; [Movie S2](#)). For comparison we coexpressed IELM-Venus with ChR2-mCherry ([Zhang et al., 2007](#)). Under the same pulsed photostimulation conditions, a similar translocation of IELM-Venus was observed within 3 hr; however, cells started to drastically shrink by 1 hr, potentially due to the passage of H⁺ through ChR2-mCherry ([Nagel et al., 2003](#)) ($n = 5/5$ cells) (Figure 4B; [Movie S3](#)). Taken together, these observations demonstrate that pulsed photostimulation of LOVS1K resulted in a sustained global Ca²⁺ signal that facilitated the translocation of IELM-Venus from the nucleoli to the PM without drastic cell shrinkage.

To confirm that global Ca²⁺ signals generated by LOVS1K can modulate different Ca²⁺-dependent proteins in different cell lines, we used LOVS1K to stop CaM-RhoA-Venus-dependent blebbing in HEK293 cells ([Mills et al., 2010](#)). RhoA regulates the formation and retraction of spherical cellular protrusions known as blebs that are thought to be the mode of cell migration during cancer metastasis ([Fackler and Grosse, 2008](#)). CaM-RhoA-Venus is an engineered Ca²⁺-sensitive RhoA protein that causes dynamic nonapoptotic bleb formation and retraction in HEK293 cells. We previously demonstrated that CaM-RhoA-Venus can be deactivated with a chemically induced increase in global intracellular Ca²⁺, resulting in bleb retraction. In HEK293 cells coexpressing LOVS1K and Orai1Ceru, blebbing slowed and eventually stopped completely within 25 min of pulsed photostimulation (300 ms exposure every 10 s; $n = 16/16$ cells) (Figures 5E and 5F; [Movie S7](#)). Cells expressing CaM-RhoA-Venus alone did not stop blebbing, even with a total of 40 min pulsed photostimulation ($n = 10/10$ cells) (Figures 5A and 5B; [Movie S5](#)). Similarly, yet surprisingly, blebbing cells ex-

pressing ChR2-mCherry did not stop blebbing despite longer pulsed photostimulation (total of 40 min; $n = 15/15$ cells) (Figures 5C and 5D; [Movie S6](#)). Taken together, these results demonstrate that repeated photostimulation of LOVS1K generated a global Ca²⁺ signal able to stop CaM-RhoA-Venus-dependent blebbing in HEK293 cells, despite previously requiring a long chemically induced Ca²⁺ transient ([Mills et al., 2010](#)) and the inability of ChR2-mCherry to stop blebbing in HEK293 cells under the same conditions.

DISCUSSION

By engineering LOV2 domain fusions with C-terminal Stim1 fragments, we have developed a reversible, photoactivated means of activating Orai1 Ca²⁺ channels to generate local Ca²⁺ signals on the PM and global Ca²⁺ signals in the cytoplasm with repeated photostimulation. Although our system is similar to ChR2 in that it does not require exogenous chemicals and can be genetically encoded, it differs in that it is specific to Ca²⁺ and does not cause intracellular pH changes. Our system could potentially be used to generate action potentials to study in vivo neural circuitry in the same way as ChR2 because it could be coupled with endogenous Ca²⁺-sensitive Cl⁻ channels ([Forrest et al., 2010](#)) and Ca²⁺-activated K⁺ channels ([Pedarzani and Stocker, 2008](#)) expressed in neurons. Because the cell lines in our study had low or no endogenous Orai1 expression, the cotransfection of both LOVS1K and Orai1Ceru was needed, but both genes could be delivered in a single open reading frame using 2A peptides ([de Felipe, 2004](#)) or a self-cleaving TEV protease ([Chen et al., 2010](#)). It is possible in cells with higher

endogenous Orai1 expression, such as lymphocytes and T cells (Hogan et al., 2010), that expressing LOVS1K alone will be sufficient to elicit Ca²⁺ influx.

Although Stim1 and Orai1 are typically associated with SOCE to generate large global Ca²⁺ influxes to replenish depleted Ca²⁺ levels (Varnai et al., 2009), our work demonstrates that another mode exists where only a local Ca²⁺ influx on the PM is generated instead. The reason for the local Ca²⁺ influx could be that Orai1 is not localized into puncta or being activated by full-length Stim1. Both of these events can conceivably be regulated by other proteins to allow Orai1 channels to generate local Ca²⁺ influxes in certain circumstances. These local Ca²⁺ influxes on the PM could expand the functionality of Orai1 by specifically modulating Ca²⁺-sensitive proteins on the PM such as Ca²⁺-sensitive Cl⁻ channels (Forrest et al., 2010) and Ca²⁺-activated K⁺ channels (Pedarzani and Stocker, 2008) without affecting Ca²⁺-sensitive proteins in other locations of the cell.

Strategies can be explored to potentially enhance the duration and extent of the photoactivated local Ca²⁺ influx. By increasing the influx of local Ca²⁺ with each photostimulation, these strategies would also lead to faster accumulation of global cytoplasmic Ca²⁺ levels. A set of reported mutations on Orai1^{Ceru} can be done to reduce the effects of inactivation by CaM or an intracellular loop within Orai1 (Mullins et al., 2009; Srikanth et al., 2010), resulting in more local Ca²⁺ influx with each photostimulation. Alternatively, mutations to the LOV2 domain can be made to increase the modest photoactivated change between the dark and bright states of LOVS1K. This can be achieved using known mutations that stabilize the dark, folded state of LOV2 domain and its J α helix, resulting in a larger dynamic range between the dark and bright states (Strickland et al., 2010). Other mutations have also been used to accelerate the transition of LOV2 back from the bright state to the dark state after photostimulation, which would accelerate the return of LOVS1K to the ground state, ready for the next photoactivation cycle (Christie et al., 2007).

The unique ability to generate local and global Ca²⁺ signals could be used to investigate the Ca²⁺ specificity problem in living organisms. For instance, in cells expressing our system, blue light could be targeted to subcellular locations such as lipid rafts and caveolae, where Ca²⁺ microdomains are initiated, to investigate the role of local Ca²⁺ signals in physiological processes such as endocytosis, exocytosis, and cell migration (Pani and Singh, 2009). Global Ca²⁺ gradients have been observed in migrating cells, opposite to the migration direction with lower Ca²⁺ levels at the front. However, generating high local Ca²⁺ microdomains at the leading edge can regulate cell polarization, directed movement, and turning of migrating cells (Wei et al., 2009). Ca²⁺ microdomains also trigger exocytosis in different cell types including synaptic vesicle release of neurotransmitters in neurons and hormones in endocrine cells (Pang and Südhof, 2010). Our system can be used to generate local Ca²⁺ signals near vesicle proteins like synaptotagmins to investigate the conditions necessary for vesicle fusion and exocytosis.

A better understanding of how Ca²⁺ can trigger specific cellular responses will facilitate the engineering of synthetic proteins that respond to specific Ca²⁺ signals. A protein with high Ca²⁺ affinity can be engineered and placed near the PM, such that it would respond selectively to high local Ca²⁺ signals.

Future potential candidates are Ca²⁺-dependent calpain proteases, which mediate cell spreading and migration. μ - and m-calpains are selectively active when localized at the PM and in the presence of either micromolar or millimolar levels of Ca²⁺, respectively (Perrin and Huttenlocher, 2002). Ca²⁺ is a remarkably versatile intracellular messenger. To facilitate research in the many different aspects of Ca²⁺ signaling, LOVS1K is a unique tool for specific photoactivation of local and global Ca²⁺ signaling that will help unravel how this ubiquitous ion orchestrates a diverse range of cellular function.

SIGNIFICANCE

Many cellular processes rely on local and global Ca²⁺ signals to maintain healthy function. The ability to controllably generate local and global Ca²⁺ signals not only facilitates the investigation of underlying Ca²⁺ signals regulating cellular processes in both healthy versus pathogenic cells, but it also aids the development of engineered synthetic proteins that respond to specific Ca²⁺ signals. Generating different Ca²⁺ signals with light is desirable because it causes minimal damage to live cells and can be precisely controlled. Light-mediated approaches to generate Ca²⁺ such as “uncaging” of molecules and photoactivation of Channelrhodopsin-2 (ChR2) have previously been reported. However, “uncaging” approaches require addition of exogenous chemicals and are not genetically encodable. Additionally, photoactivation of Ca²⁺ channels allows a greater influx of Ca²⁺ ions compared to “uncaging” approaches. ChR2 is genetically encodable but has its own drawbacks. These include being permeable to H⁺, which may have detrimental effects on intracellular pH, and not being selective for Ca²⁺. LOVS1K presents a better alternative for generating Ca²⁺ signals because it is genetically encoded, is highly selective for Ca²⁺ transport, and can reversibly generate a local Ca²⁺ signal on the PM or a global Ca²⁺ signal with repeated photostimulation. We have used LOVS1K to modulate engineered Ca²⁺-inducible proteins, showing that LOVS1K can modulate these engineered proteins better than ChR2 without cell shrinkage in long time course experiments.

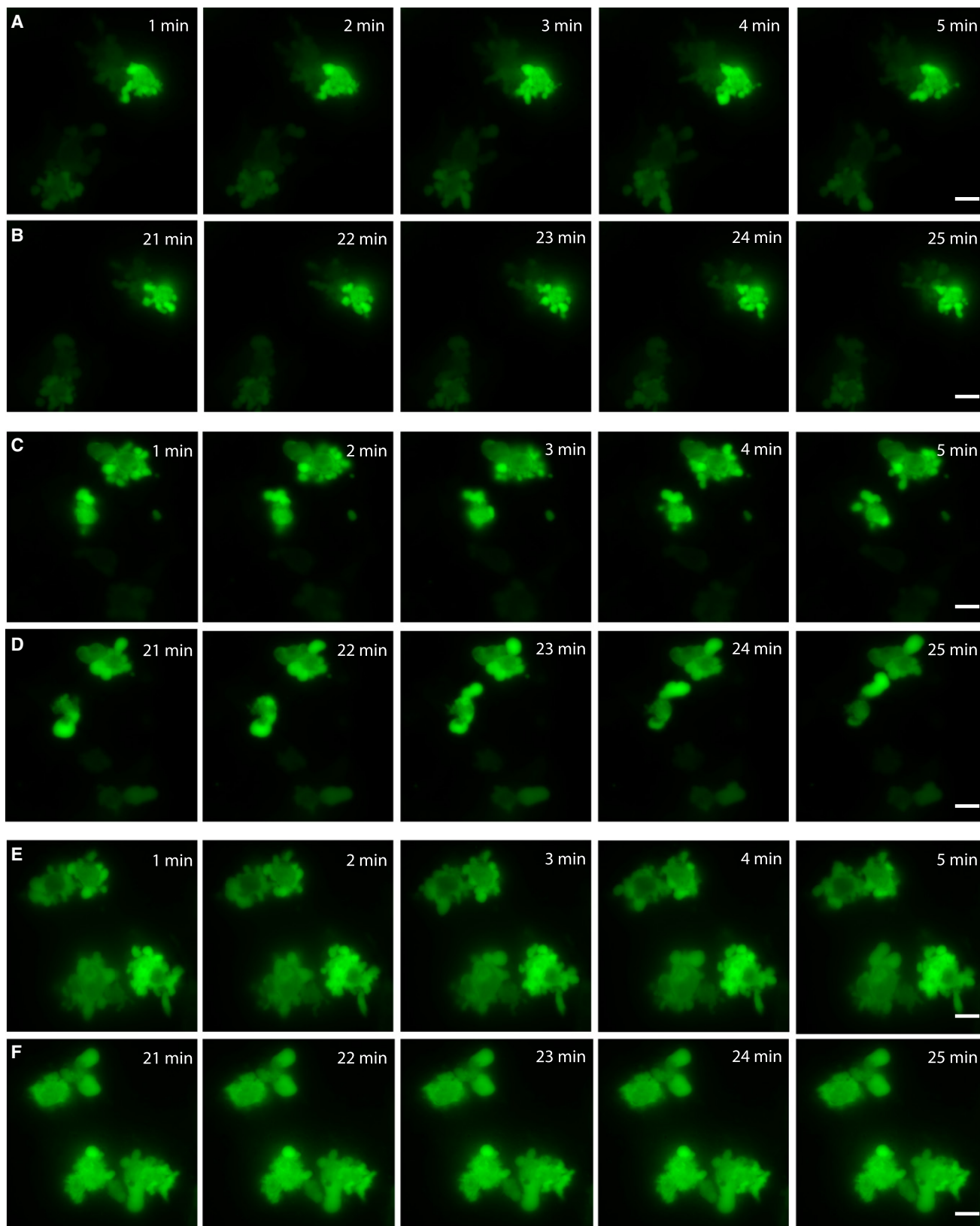
EXPERIMENTAL PROCEDURES

Plasmids

LOV2, Stim1, Orai1, and ChR2-mCherry were from Addgene plasmids 22027, 19754, 19756, and 20938, respectively (Cambridge, MA, USA). All subcloning was performed as described (Pham and Truong, 2010; Truong et al., 2003). The LOV2-J α domain, Stim1 fragments, and Orai1 were amplified and inserted into pCfVtx3 (Truong et al., 2003). The Venus was removed and replaced with either Cerulean or mRFP to make: S1K (233–450), S2K (233–474), S3K (342–450), S4K (342–474), S5K (233–420), and Orai1^{Ceru}. LOV2-J α was inserted at the N terminus to make LOVS1K, LOVS2K, LOVS3K, and LOVS4K. LOV2-J α point mutations (Cys450Ala and Ile539Glu) were made to create darkLOVS1K and brightLOVS1K, respectively. TNXL (Mank et al., 2006) was subcloned with a PM localization tag pLyn, from Lyn kinase (GCIKSKGKDSA), to make pLynTNXL.

Cell Culture and Transfection

Cos-7, HEK293, HeLa, and NIH 3T3 cells were maintained in Dulbecco's modified Eagle's medium containing 25 mM D-glucose, 1 mM sodium pyruvate,



and 4 mM L-glutamine (Invitrogen, Carlsbad, CA) with 10% supplemented fetal bovine serum (FBS) (Sigma-Aldrich, St. Louis, MO) in T5 flasks (37°C and 5% CO₂). Cells were passaged at 95% confluency using 0.05% Trypsin with EDTA (Sigma-Aldrich) and seeded onto 35 mm glass-bottom dishes (MatTek, Ashland, MA) at 1:15 dilution. Cells were transiently transfected using Lipofectamine 2000 according to manufacturer's protocols (Invitrogen).

Illumination and Imaging

Imaging was performed using an inverted IX81 microscope with Lambda DG4 xenon lamp source and QuantEM 512SC CCD camera with a 60× oil immersion objective (Olympus). Filter EX and EM band-pass specifications were as follows: CFP (EX: 438/24 nm, EM: 482/32 nm); YFP (EX: 500/24 nm, EM: 542/27 nm); and RFP (EX: 580/20 nm, EM: 630/60 nm) (Semrock). To photostimulate LOV2 constructs and ChR2-mCherry, CFP EX was used. For repeated photostimulation of LOV2 constructs, CFP EX was illuminated for 300 ms every 10 s. FRET measurements were collected using CFP EX with a dual-band filter (480 nm/30 nm and 535 nm/30 nm, 505 nm beamsplitter dichroic mirror, Photometrics DV2) to simultaneously collect CFP and YFP EM. The light intensity was 25 mW/mm². Image acquisition was done with MetaMorph Advanced (Olympus).

Quantification of Colocalization

PC values range between -1 and 1, with -1 representing exclusion and 1 representing complete colocalization. However, between these extremes it is difficult to interpret partial colocalization patterns and intermediate PC values. To distinguish between true partial colocalization and random overlap, van Steensel's CCFs provide PC values with a measure of statistical significance (van Steensel et al., 1996). van Steensel's method calculates CCF values while shifting one image relative to the other and plotting these as a function of displacement. This method does not depend on the relative intensities of the two fluorescent signals. CCF plots show a bell-shaped curve for true colocalization and a dip for exclusion. Complete colocalization would show a peak at zero, whereas partial colocalization would show a bell-shaped curve with a nonzero peak. These peak CCF values indicate the fraction of colocalization between two images, with higher peaks (values closer to 1) corresponding to more colocalization (Nahrendorf et al., 2010; van Steensel et al., 1996). PCs were calculated using the JACoP plug-in available with ImageJ (Bolte and Cordelières, 2006). Thresholded PCs were additionally calculated to objectively minimize any effects of noise in the images. van Steensel's statistically determined CCF values were also calculated for each case (van Steensel et al., 1996).

SUPPLEMENTAL INFORMATION

Supplemental Information includes four figures, two tables, and seven movies and can be found with this article online at doi:10.1016/j.chembiol.2011.04.014.

ACKNOWLEDGMENTS

This work was made possible by plasmid sharing through Addgene, particularly by K.M. Hahn for depositing PA-Rac, K. Deisseroth for ChR2, and A. Rao for Stim1 and Orai1. We also thank S. Nagaraj for help with plasmid construction. This work was supported by fellowships to E.P. and E.M. from the Natural Science and Engineering Research Council (NSERC) and a grant to K.T. from the Canadian Institutes of Health Research (#81262). E.P. designed and carried out experiments, created plasmids used, analyzed the data, and wrote the manuscript. E.M. produced plasmids used in the work

and performed control experiments. K.T. conceived the initial idea, analyzed the data, and helped write the manuscript.

Received: January 16, 2011

Revised: April 4, 2011

Accepted: April 22, 2011

Published: July 28, 2011

REFERENCES

- Airan, R.D., Thompson, K.R., Fenno, L.E., Bernstein, H., and Deisseroth, K. (2009). Temporally precise in vivo control of intracellular signalling. *Nature* 458, 1025–1029.
- Berridge, M.J., Lipp, P., and Bootman, M.D. (2000). The versatility and universality of calcium signalling. *Nat. Rev. Mol. Cell Biol.* 1, 11–21.
- Berridge, M.J., Bootman, M.D., and Roderick, H.L. (2003). Calcium signalling: dynamics, homeostasis and remodelling. *Nat. Rev. Mol. Cell Biol.* 4, 517–529.
- Bi, A., Cui, J., Ma, Y.P., Olshevskaya, E., Pu, M., Dizhoor, A.M., and Pan, Z.H. (2006). Ectopic expression of a microbial-type rhodopsin restores visual responses in mice with photoreceptor degeneration. *Neuron* 50, 23–33.
- Bolte, S., and Cordelières, F.P. (2006). A guided tour into subcellular colocalization analysis in light microscopy. *J. Microsc.* 224, 213–232.
- Boyden, E.S., Zhang, F., Bamberg, E., Nagel, G., and Deisseroth, K. (2005). Millisecond-timescale, genetically targeted optical control of neural activity. *Nat. Neurosci.* 8, 1263–1268.
- Bruegmann, T., Malan, D., Hesse, M., Beiert, T., Fuegemann, C.J., Fleischmann, B.K., and Sasse, P. (2010). Optogenetic control of heart muscle in vitro and in vivo. *Nat. Methods* 7, 897–900.
- Calloway, N., Holowka, D., and Baird, B. (2010). A basic sequence in STIM1 promotes Ca²⁺ influx by interacting with the C-terminal acidic coiled coil of Orai1. *Biochemistry* 49, 1067–1071.
- Chen, X., Pham, E., and Truong, K. (2010). TEV protease-facilitated stoichiometric delivery of multiple genes using a single expression vector. *Protein Sci.* 19, 2379–2388.
- Christie, J.M., Corchnoy, S.B., Swartz, T.E., Hokenson, M., Han, I.S., Briggs, W.R., and Bogomolni, R.A. (2007). Steric interactions stabilize the signaling state of the LOV2 domain of phototropin 1. *Biochemistry* 46, 9310–9319.
- Costes, S.V., Daelemans, D., Cho, E.H., Dobbin, Z., Pavlakis, G., and Lockett, S. (2004). Automatic and quantitative measurement of protein-protein colocalization in live cells. *Biophys. J.* 86, 3993–4003.
- de Felipe, P. (2004). Skipping the co-expression problem: the new 2A "CHYSEL" technology. *Genet. Vaccines Ther.* 2, 13.
- Ellis-Davies, G.C. (2007). Caged compounds: photorelease technology for control of cellular chemistry and physiology. *Nat. Methods* 4, 619–628.
- Fackler, O.T., and Grosse, R. (2008). Cell motility through plasma membrane blebbing. *J. Cell Biol.* 181, 879–884.
- Feldbauer, K., Zimmermann, D., Pintschovius, V., Spitz, J., Bamann, C., and Bamberg, E. (2009). Channelrhodopsin-2 is a leaky proton pump. *Proc. Natl. Acad. Sci. USA* 106, 12317–12322.
- Forrest, A.S., Angermann, J.E., Raghunathan, R., Lachendro, C., Greenwood, I.A., and Leblanc, N. (2010). Intricate interaction between store-operated calcium entry and calcium-activated chloride channels in pulmonary artery smooth muscle cells. *Adv. Exp. Med. Biol.* 667, 31–55.

Figure 5. CaM-RhoA-Venus-Dependent Blebbing Stopped with Repeated Photoactivation of LOVS1K, but Not ChR2-mCherry

(A and B) HEK293 cells expressing CaM-RhoA-Venus were blebbing and did not stop blebbing with 25 min of pulsed photostimulation (n = 2 experiments and 10/10 observed cells).

(C and D) Blebbing HEK293 cells coexpressing ChR2-mCherry did not stop blebbing with 25 min of pulsed photostimulation (n = 3 experiments and 15/15 observed cells).

(E and F) HEK293 cells coexpressing LOVS1K and Orai1 Ceru were blebbing at the start of the experiment. By the end of 25 min of pulsed photostimulation, cells had stopped blebbing (n = 3 experiments and 16/16 observed cells). Early time points (1–5 min) and later time points (21–25 min) are shown for comparison. Scale bars represent 30 μm. Images are false color: CaM-RhoA-Venus, green.

See also Movie S5, Movie S6, and Movie S7.

- Frischauf, I., Muik, M., Derler, I., Bergsmann, J., Fahrner, M., Schindl, R., Groschner, K., and Romanin, C. (2009). Molecular determinants of the coupling between STIM1 and Orai channels: differential activation of Orai1-3 channels by a STIM1 coiled-coil mutant. *J. Biol. Chem.* **284**, 21696–21706.
- Gradinaru, V., Zhang, F., Ramakrishnan, C., Mattis, J., Prakash, R., Diester, I., Goshen, I., Thompson, K.R., and Deisseroth, K. (2010). Molecular and cellular approaches for diversifying and extending optogenetics. *Cell* **141**, 154–165.
- Harper, S.M., Christie, J.M., and Gardner, K.H. (2004). Disruption of the LOV-Jalpha helix interaction activates phototropin kinase activity. *Biochemistry* **43**, 16184–16192.
- Heim, N., and Griesbeck, O. (2004). Genetically encoded indicators of cellular calcium dynamics based on troponin C and green fluorescent protein. *J. Biol. Chem.* **279**, 14280–14286.
- Hogan, P.G., Lewis, R.S., and Rao, A. (2010). Molecular basis of calcium signaling in lymphocytes: STIM and ORAI. *Annu. Rev. Immunol.* **28**, 491–533.
- Inoue, T., Heo, W.D., Grimley, J.S., Wandless, T.J., and Meyer, T. (2005). An inducible translocation strategy to rapidly activate and inhibit small GTPase signaling pathways. *Nat. Methods* **2**, 415–418.
- Kravitz, A.V., Freeze, B.S., Parker, P.R., Kay, K., Thwin, M.T., Deisseroth, K., and Kreitzer, A.C. (2010). Regulation of parkinsonian motor behaviours by optogenetic control of basal ganglia circuitry. *Nature* **466**, 622–626.
- Li, Q., Lau, A., Morris, T.J., Guo, L., Fordyce, C.B., and Stanley, E.F. (2004). A syntaxin 1, Galph(o), and N-type calcium channel complex at a presynaptic nerve terminal: analysis by quantitative immunocolocalization. *J. Neurosci.* **24**, 4070–4081.
- Manders, E.M., Stap, J., Brakenhoff, G.J., van Driel, R., and Aten, J.A. (1992). Dynamics of three-dimensional replication patterns during the S-phase, analysed by double labelling of DNA and confocal microscopy. *J. Cell Sci.* **103**, 857–862.
- Mank, M., Reiff, D.F., Heim, N., Friedrich, M.W., Borst, A., and Griesbeck, O. (2006). A FRET-based calcium biosensor with fast signal kinetics and high fluorescence change. *Biophys. J.* **90**, 1790–1796.
- McNally, B.A., Yamashita, M., Engh, A., and Prakriya, M. (2009). Structural determinants of ion permeation in CRAC channels. *Proc. Natl. Acad. Sci. USA* **106**, 22516–22521.
- Mills, E., and Truong, K. (2010). Engineering Ca²⁺/calmodulin-mediated modulation of protein translocation by overlapping binding and signaling peptide sequences. *Cell Calcium* **47**, 369–377.
- Mills, E., Pham, E., and Truong, K. (2010). Structure based design of a Ca²⁺-sensitive RhoA protein that controls cell morphology. *Cell Calcium* **48**, 195–201.
- Mullins, F.M., Park, C.Y., Dolmetsch, R.E., and Lewis, R.S. (2009). STIM1 and calmodulin interact with Orai1 to induce Ca²⁺-dependent inactivation of CRAC channels. *Proc. Natl. Acad. Sci. USA* **106**, 15495–15500.
- Nagel, G., Szellas, T., Huhn, W., Kateriya, S., Adeishvili, N., Berthold, P., Ollig, D., Hegemann, P., and Bamberg, E. (2003). Channelrhodopsin-2, a directly light-gated cation-selective membrane channel. *Proc. Natl. Acad. Sci. USA* **100**, 13940–13945.
- Nagel, G., Brauner, M., Liewald, J.F., Adeishvili, N., Bamberg, E., and Gottschalk, A. (2005). Light activation of channelrhodopsin-2 in excitable cells of *Caenorhabditis elegans* triggers rapid behavioral responses. *Curr. Biol.* **15**, 2279–2284.
- Nahrendorf, M., Keliher, E., Marinelli, B., Waterman, P., Feruglio, P.F., Fexon, L., Pivovarov, M., Swirski, F.K., Pittet, M.J., Vinegoni, C., et al. (2010). Hybrid PET-optical imaging using targeted probes. *Proc. Natl. Acad. Sci. USA* **107**, 7910–7915.
- Pang, Z.P., and Südhof, T.C. (2010). Cell biology of Ca²⁺-triggered exocytosis. *Curr. Opin. Cell Biol.* **22**, 496–505.
- Pani, B., and Singh, B.B. (2009). Lipid rafts/caveolae as microdomains of calcium signaling. *Cell Calcium* **45**, 625–633.
- Parekh, A. (2007). Intracellular Ca²⁺ signaling: calcium influx. In *Calcium Signaling: Regulation, Mechanisms, Effectors, Role in Disease and Recent Advances*, A. Simpson, ed. (London: The Biomedical & Life Sciences Collection, Henry Stewart Talks Ltd) (<http://www.hstalks.com>).
- Parekh, A.B. (2009). Local Ca²⁺ influx through CRAC channels activates temporally and spatially distinct cellular responses. *Acta Physiol. (Oxf.)* **195**, 29–35.
- Pedarzani, P., and Stocker, M. (2008). Molecular and cellular basis of small- and intermediate-conductance, calcium-activated potassium channel function in the brain. *Cell. Mol. Life Sci.* **65**, 3196–3217.
- Perrin, B.J., and Huttenlocher, A. (2002). Calpain. *Int. J. Biochem. Cell Biol.* **34**, 722–725.
- Pham, E., and Truong, K. (2010). Design of fluorescent fusion protein probes. *Methods Mol. Biol.* **591**, 69–91.
- Salomon, M., Christie, J.M., Knieb, E., Lempert, U., and Briggs, W.R. (2000). Photochemical and mutational analysis of the FMN-binding domains of the plant blue light receptor, phototropin. *Biochemistry* **39**, 9401–9410.
- Schindl, R., Muik, M., Fahrner, M., Derler, I., Fritsch, R., Bergsmann, J., and Romanin, C. (2009). Recent progress on STIM1 domains controlling Orai activation. *Cell Calcium* **46**, 227–232.
- Srikanth, S., Jung, H.J., Ribalet, B., and Gwack, Y. (2010). The intracellular loop of Orai1 plays a central role in fast inactivation of Ca²⁺ release-activated Ca²⁺ channels. *J. Biol. Chem.* **285**, 5066–5075.
- Strickland, D., Moffat, K., and Sosnick, T.R. (2008). Light-activated DNA binding in a designed allosteric protein. *Proc. Natl. Acad. Sci. USA* **105**, 10709–10714.
- Strickland, D., Yao, X., Gawlak, G., Rosen, M.K., Gardner, K.H., and Sosnick, T.R. (2010). Rationally improving LOV domain-based photoswitches. *Nat. Methods* **7**, 623–626.
- Tadross, M.R., Dick, I.E., and Yue, D.T. (2008). Mechanism of local and global Ca²⁺ sensing by calmodulin in complex with a Ca²⁺ channel. *Cell* **133**, 1228–1240.
- Truong, K., Khorchid, A., and Ikura, M. (2003). A fluorescent cassette-based strategy for engineering multiple domain fusion proteins. *BMC Biotechnol.* **3**, 8.
- van Steensel, B., van Binnendijk, E.P., Hornsby, C.D., van der Voort, H.T., Krozowski, Z.S., de Kloet, E.R., and van Driel, R. (1996). Partial colocalization of glucocorticoid and mineralocorticoid receptors in discrete compartments in nuclei of rat hippocampus neurons. *J. Cell Sci.* **109**, 787–792.
- Varnai, P., Hunyady, L., and Balla, T. (2009). STIM and Orai: the long-awaited constituents of store-operated calcium entry. *Trends Pharmacol. Sci.* **30**, 118–128.
- Wei, C., Wang, X., Chen, M., Ouyang, K., Song, L.S., and Cheng, H. (2009). Calcium flickers steer cell migration. *Nature* **457**, 901–905.
- Woodard, G.E., Salido, G.M., and Rosado, J.A. (2008). Enhanced exocytotic-like insertion of Orai1 into the plasma membrane upon intracellular Ca²⁺ store depletion. *Am. J. Physiol. Cell Physiol.* **294**, C1323–C1331.
- Wu, Y.I., Frey, D., Lungu, O.I., Jaehrig, A., Schlichting, I., Kuhlman, B., and Hahn, K.M. (2009). A genetically encoded photoactivatable Rac controls the motility of living cells. *Nature* **461**, 104–108.
- Yu, F., Sun, L., and Machaca, K. (2009). Orai1 internalization and STIM1 clustering inhibition modulate SOCE inactivation during meiosis. *Proc. Natl. Acad. Sci. USA* **106**, 17401–17406.
- Yu, F., Sun, L., and Machaca, K. (2010). Constitutive recycling of the store-operated Ca²⁺ channel Orai1 and its internalization during meiosis. *J. Cell Biol.* **191**, 523–535.
- Zhang, F., Wang, L.P., Brauner, M., Liewald, J.F., Kay, K., Watzke, N., Wood, P.G., Bamberg, E., Nagel, G., Gottschalk, A., et al. (2007). Multimodal fast optical interrogation of neural circuitry. *Nature* **446**, 633–639.
- Zhou, Y., Ramachandran, S., Oh-Hora, M., Rao, A., and Hogan, P.G. (2010). Pore architecture of the ORAI1 store-operated calcium channel. *Proc. Natl. Acad. Sci. USA* **107**, 4896–4901.